RSC Advances

ROYAL SOCIETY OF CHEMISTRY

www.rsc.org/advances

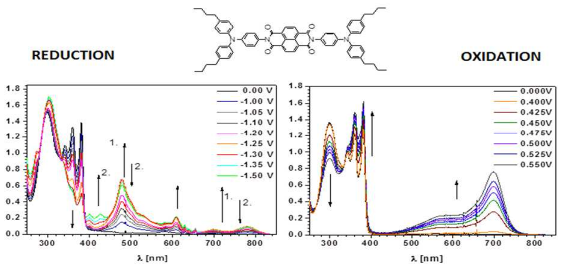

The ambipolar behavior of group of N-substituted and core-functionalized with triarylamine arylene bisimeds were investigated by electrochemical and spectroelectrochemical (UV-Vis and EPR spectroelectrochemistry) technics.

UV-vis and EPR spectroelectrochemical investigations of triaryl amine functionalized arylene bisimides

Sandra Pluczyk[1], Pawel Zassowski[1], Renata Rybakiewicz[2], Renata Wielgosz[2], Malgorzata Zagorska[2], Mieczyslaw Lapkowski[1,3]* and Adam Pron[2]**

[1]Silesian University of Technology, Faculty of Chemistry, Strzody 9, 44-100 Gliwice, Poland
[2]Faculty of Chemistry, Warsaw University of Technology, Noakowskiego 3, 00-664 Warsaw, Poland
[3]Centre of Polymer and Carbon Materials, Polish Academy of Sciences, M. Curie-Sklodowska 34, 41-819 Zabrze, Poland

Abstract

Four arylene bisimides N-substituted with triarylamine and three bisimides core-functionalized with the same substituent were studied by cyclic voltammetry, UV-vis and EPR spectroelectrochemistry. All investigated compounds showed ambipolar behaviour manifested by their *quasi*-reversible reduction to radical anions and *quasi*-reversible oxidation to radical cations. The presence of stable radical anions and radical cations was confirmed by EPR spectroelectrochemical experiments. Formation of the radical anions resulted in bleaching of the bisimide UV-vis bands with simultaneous hypsochromic shift of the charge transfer (CT) band and appearance of the radical anion peaks, the bands originating from the triarylamine remaining essentially unchanged. Electrochemical generation of radical cations resulted in turn in bleaching of the triarylamine band accompanied by a hypsochromic shift of the CT band and with the appearance of the radical cation bands at higher wavelengths, the bisimide bands remaining essentially intact.

Introduction

Functionalized arylene bisimides have been used for many years as different types of dyes.[1]
More recently, they have been applied as active layers in n-channel organic field effect transistors (OFETs)[2–8] or as building blocks in photochromic and electrochemically-active metal-organic frameworks.[9–13] One of the advantages of these organic semiconductors is the possibility of tuning their electron affinity (EA) through core or imide nitrogen functionalization with appropriate electron accepting (donating) groups.[5,14–18]
Low and high molecular mass triarylamines are in turn very suitable for the fabrication of active layers in p-channel FETs or as hole conducting materials, in general (see for example[19]

and references therein) or as electrochromic[20] and electrofluorochromic[21] materials. In their oxidized states they also frequently serve as spin-carrying units in high spin organic materials due to good stability of their radical cation form which in molecules of appropriate topology facilitates ferromagnetic spin coupling.[22]

Molecules (macromolecules) combining triarylamine and arylene bisimide moieties connected either directly or through appropriate linkers have been designed and studied in the past decade as components of electrochromic materials and/or materials showing volatile and non-volatile memory.[23–29] In addition many compounds of this family exhibit ambipolar properties which are scarce and still greatly in demand. Several solution processable arylene bisimides N- or core-substituted with triarylamines have been synthesized.[17,30,31] In addition to being attractive organic semiconductors, yielding ambipolar OFETs operating in air,[17,31] they show interesting and reversible electrochemical behaviour.[32]

In this work we describe the results of UV-vis and EPR spectroelectrochemical investigations of arylene bisimides differently substituted with triarylamine. No such data have ever been reported and their publication is interesting because they form stable radical ions both in their oxidized and reduced forms, whose electronic structure is dependent on the size of the bisimide core as well as on the number and positions of triarylamine substituents.

Experimental

Synthesis

The preparation procedures of already published bisimides (**B1, B2** and **B3**) can be found in *Electronic Supplementary Information* (*ESI*) of ref.[30] whereas that of **B4** in ref.[31] and **B5** in ref.[32] The detailed synthetic pathways leading to **B6** and **B7**, together with their spectroscopic characterization, can be found in the *Supplementary Information* of this paper.

Cyclic voltammetry

Cyclic voltammograms of the synthesized compounds were registered using an Autolab potentiostat (EcoChemie) in the electrolytic medium consisting of the studied bisimide dissolved in 0.1 M dichloromethane solution of Bu_4NBF_4. The measurements were performed in an inert atmosphere, using a platinum working electrode of the surface area of 3 mm^2, a platinum wire counter electrode and an Ag/0.1 M Ag^+ reference electrode consisting of an Ag wire immersed in 0.1 M solution of $AgNO_3$ in acetonitrile.

UV-vis and EPR spectroelectrochemistry

The spectroelectrochemical cell used in the UV-vis spectroelectrochemical investigations was a modification of cells described in[33–35]. In all experiments 10^{-4} M solution of a given bisimide was prepared in 0.1 M Bu_4NPF_6/dichloromethane electrolyte. The spectra were recorded in a 2 mm thick cuvette using an UV-Vis Hewlett Packard 8453 spectrometer. The platinum mesh was used as a working electrode, a platinum spiral as an auxiliary electrode and a silver wire as a pseudo-reference electrode. In the case of solid state spectroelectrochemistry, thin films of a given compound were deposited on an ITO electrode by casting from solution. In this case, dichloromethane was replaced by acetonitrile.

Electrochemical cells of several different geometries can be envisioned for EPR spectroelectrochemical investigations[34], the majority of them being flat[36,37]. In this research a cylindrical cell was used, similar to that described in[38] and identical to the cell reported in [39]. In particular, EPR measurements were carried out in 10^{-3}M solution of an investigated bisimide in 0.1 M Bu_4NPF_6/dichloromethane electrolyte using a cylindrical custom - made cell equipped with a platinum wire working electrode, an auxiliary electrode in a form of platinum spiral and a silver wire as a pseudo - reference electrode. The pseudo-reference electrode potential was checked after each experiment by recording a cyclic voltammogram of ferrocene added to the same electrolyte solution. The experiments were performed using a JEOL JES-FA 200, X-band CW-EPR spectrometer operating at 100 kHz field modulation. EPR spectra of the electrochemically generated radicals were fitted using WinSim software[40] G-factor was estimated by comparison with JEOL spectrometer internal standard (Mn(II) salt in quartz tube).

DFT/TDDFT calculations

DFT/TDDFT calculations have been carried with B3LYP[41–43] hybrid functional with 6-31G(d) basis set. Ground state geometry was optimized without symmetry constraints to a local minimum, which was followed by frequency calculations. Alkyl chains were cut to the methyl group, in order to speed up the calculations. No imaginary frequencies were detected, which proved that obtained geometry was a local minimum. All calculations were carried out with a polarizable continuum model,[44] using dichloromethane as a solvent in order to simulate the solution effects. All calculations were carried out with Gaussian 09 software.[45] Input files and plots were prepared with Gabedit software.[46]

Results and discussion

The investigated compounds are depicted in Chart 1. They can be divided into two groups, imide nitrogen - (**B1, B2, B3, B4)** and core - (**B5, B6, B7)** substituted derivatives.

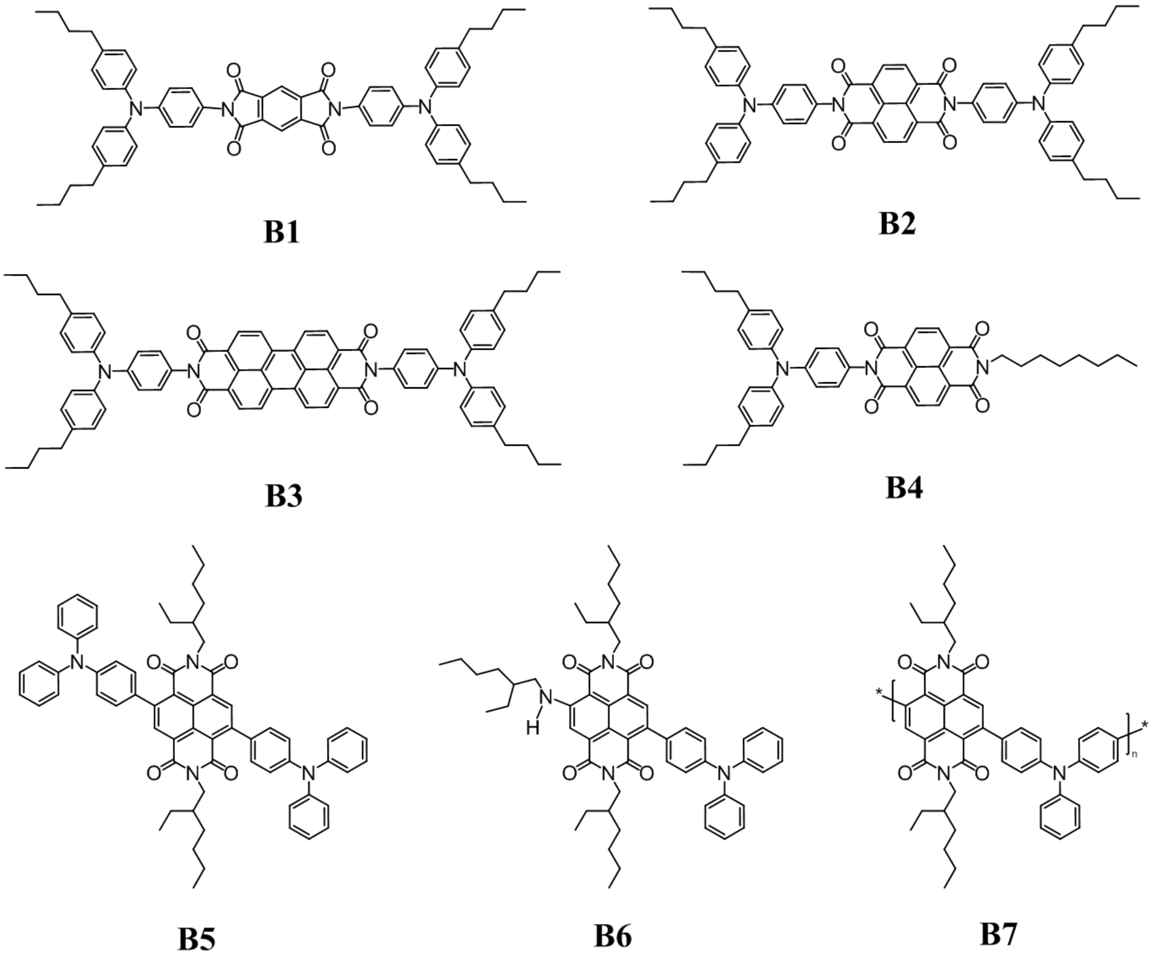
B1 **B2** **B3** **B4** **B5** **B6** **B7**

Chart 1. Chemical formulae of triarylamine-substituted arylene bisimides studied.

Cyclic voltammetry

Representative voltammograms of N- and core-substituted arylene bisimides (**B2** and **B5)** are shown in **Fig. 1.** Voltammograms of the remaining compounds can be found in **Fig. S1.** of *Supporting Information*. Redox potentials of all studied compounds, derived from the cyclic voltammetry data, are listed in **Tables 1** and **2.**

The electrochemical features of the registered voltammograms require some comments. In core-substituted bisimides, the peak to peak separation of the forward and reversed waves in the bisimide reduction process is equal to *ca.* 70 to 80 mV, in line with the corresponding value measured in the same conditions for the ferrocene redox couple. These values exceed by

10 to 20 mV the theoretical ones and reflect higher resistivity of non-aqueous electrolytes used in this research as compared to aqueous ones. In N-substituted compounds this separation is even higher (from 100 V to 130 mV) which is evidently associated with slower kinetics of the electron transfer in these derivatives. For the triarylamine oxidation process the separation of peaks is comparable for both types of compounds (from 70 mV to 110 nm) with the exception of **B7** where a larger separation is measured (see **Table 2**).

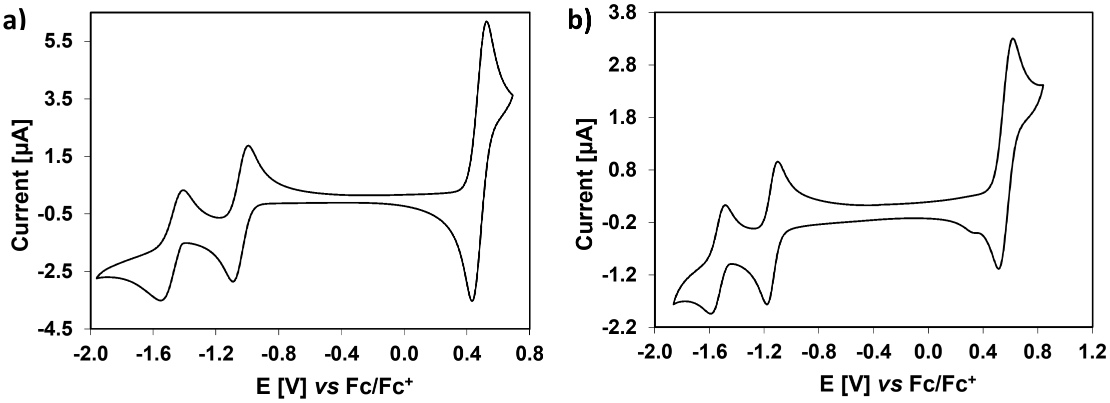

Fig. 1. Cyclic voltammograms of: **B2 (a)** and **B5 (b).** Concentration of **B2**: 1 × 10^{-3} M and **B5**: 5 × 10^{-4}M**;** electrolyte 0.1M Bu_4NBF_4 in CH_2Cl_2; scan rate 50 mV/s.

The presented voltammograms reflect the mechanism of arylene bisimide reduction.[47] For naphthalene and perylene bisimides the two reduction peaks, observed at negative potentials (Ered1 and Ered2) are associated with the successive reduction of the two imide groups to a radical cation in the first stage and to a dianion in the second stage. The first reduction step leads to an increase of the electron density on the arylene core. Thus, the addition of a second electron in the consecutive reduction step is determined by the capability of delocalizing the surplus electron density, imposed on the core during the first reduction step. This capability is strongly dependent on the size of the core. For this reason ΔE = Ered1 – Ered2 is lower for **B3** than for **B2**. In bisimides of even larger cores like in quaterrylene ones, for example, the two reduction peaks merge into one peak of doubled intensity, indicating that both reduction steps described above occur at the same potential.[47] For the same reason the reduction of the smallest core bisimide **(B1)** is limited to the first reduction step only since the surplus electron density in the formed radical anion cannot be efficiently delocalized (see **Table 1** and **Fig. S1**).

In N-substituted bisimides the potential of the first reduction peak increases from **B1** to **B3**, indicating greater facility of larger cores to accept an extra electron. It should be also pointed out that bisimides of the same core, *eg.* naphthalene bisimides, but differently N-substituted with triarylamine (**B2** and **B4**) undergo the first and the second reduction at very similar potentials **(Table 1)**. These findings corroborate the results of DFT calculations presented in refs[30] and[31] which, for N-substituted bisimides, show orthogonality of the triarylamine phenylene ring attached to imide nitrogen with respect to the plane of the bisimide core and by consequence no conjugation between the substituent and the core. Moreover, they also indicate separation of the frontier orbitals in space with HOMO being located on the triarylamine substituent whereas LUMO – on the bisimide core.

Core-functionalized arylene bisimides are more difficult to reduce. The formal potential of the first redox couple ($E^0{}_1$ = 1/2(Ered1 + Eox1)) of **B5** is shifted to lower values by 90 mV as compared to the case of **B2** in which the triarylamine substituents are attached to the imide nitrogen atoms. This is consistent with DFT calculations of core-substituted arylene bisimides reported in ref.[17] In N-substituted bisimides no or a negligible electron donating effect of triarylamine is observed due to orthogonality of the bisimide core and the substituent phenyl ring attached to bisimide nitrogen. In the case of core-substituted compounds the electron donating effect of triarylamine is observed, leading to an increase of the LUMO level energy which is manifested by the already mentioned decrease of the first reduction peak potential. This effect is amplified in **B6** where a secondary amine group is attached directly to the core in addition to the triarylamine substituent (see **Table 1**).

The *quasi*-reversible redox couple at positive potentials corresponds to the oxidation of the triarylamine moiety to a radical cation and its consecutive reduction to the neutral form. Note that for triarylamine disubstituted arylene bisimides only one oxidation peak is registered, similarly like in the case of derivatives with only one triarylamine substituent. This means that the oxidation of both substituents occurs concomitantly at the same potential. This is additionally corroborated by the integration of the peaks corresponding to the formation of the radical anion and the radical cation, respectively. In the case of N-substituted derivatives (**B1-B4**), the formal potential of this redox couple ($E^0{}_3$ = 1/2(Eox3 + Ered3)) is essentially independent of the core-size, clearly corroborating previous DFT calculations again indicating orthogonality of the core and the substituent and the lack of conjugation (see Table 2). Triarylamine groups in core-substituted derivatives (**B5-B7)** are more difficult to oxidize than in the N-substituted ones (**B1-B4),** reflecting the electron accepting effect of the bisimide moiety on the triarylamine substituent, again in accordance with previous DFT calculations.[17,31]

Table 1 Redox potentials vs Fc/Fc$^+$ of the studied triarylamine-substituted arylene bisimides in the negative potentials range

Compound	Ered1 (V)	Eox1 (V)	1/2(Ered1 + Eox1) (V)	Ered1(onset) (V)	Ered2 (V)	Eox2 (V)
B1	-1.32	-1.19	-1.26	-1.16	-	-
B2	-1.10	-1.00	-1.05	-0.97	-1.55	-1.41
B3	-1.07	-0.96	-1.02	-0.96	-1.25	-1.15
B4	-1.13	-1.01	-1.07	-1.00	-1.59	-1.42
B5	-1.18	-1.10	-1.14	-1.06	-1.59	-1.49
B6	-1.37	-1.29	-1.33	-1.26	-1.80	-1.67
B7	-1.19	-1.11	-1.15	-1.05	-1.57	-1.51

Table 2 Redox potentials vs Fc/Fc+ of the studied triarylamine-substituted arylene bisimides in the positive potentials range

Compound	Eox3 (V)	Ered3 (V)	1/2(Eox3 + Ered3) (V)	Eox3 (onset) (V)
B1	0.52	0.42	0.47	0.40
B2	0.53	0.43	0.48	0.39
B3	0.50	0.41	0.46	0.37
B4	0.53	0.42	0.48	0.41
B5	0.62	0.51	0.56	0.48
B6	0.56	0.49	0.53	0.44
B7	0.62	0.48	0.55	0.42

UV-vis spectroscopy

UV-vis spectra of N-substituted arylene bisimides (**B1** – **B4)** have some common features: i) a strong band in the vicinity of 300 nm characteristic of the triarylamine substituent. The position of this band is independent of the size of the bisimide core (see **Table 3**): ii) a band at higher wavelengths, corresponding to the $\pi-\pi^*$ transition in the bisimide core. Its position and its relative intensity with respect to the triarylamine band are dependent on the core size. In the case of **B1** (pyromellitic bisimide) this band strongly overlaps with the triarylamine band. For **B2-B4** it shows a clear vibrational structure with the peak originating from the *0-0* transition being the most intensive. A representative spectrum of this group of bisimides (**B2**) is shown in **Fig. 2a** whereas the spectra of other bisimides of this group can be found in **Fig. S2** of *Supporting Information*. All these spectra can be considered as a superposition the spectrum of "free" triarylamine and that of the corresponding arylene bisimide containing non-chromophoric N-substituents, for example alkyl groups.[48] This again supports previous DFT calculations which indicate no conjugation between the substituent and the core.[30,31]

The spectra of core-substituted bisimides are significantly different. A representative spectrum of this group of bisimides **(B5)** is shown in **Fig. 2b.** It shows a new broad band, nonexistent in the spectra of N-substituted bisimides, with a maximum at 592 nm, whose presence is associated with a charge transfer (CT)-type transition between the triarylamine and the bisimide core which are directly connected.[49–52] The band of vibronic nature, originating from the π–π* transition of the bisimide core, is significantly altered, as compared to the case of N-substituted bisimides. The lines corresponding to particular transitions are broadened: the *0-2* transition at 339 nm becomes dominant, with the *0-1* one present as a shoulder and the *0-0* transition giving rise to a weak peak at 381 nm. The peak characteristic of the triarylamine moiety is bathochromically shifted to 309 nm, *i.e.* by *ca*. 10 nm as compared to the corresponding band in N-substituted bisimides. All these changes reflect the presence of donor-acceptor interactions in core-functionalized bisimides, predicted by DFT calculations.[17] These interactions not only influence the spectral properties of these compounds but also alter their oxidation and reduction potentials (*vide supra*). UV-vis spectra of other bisimides of this group can be found in **Fig. S3** of *Supporting Information*.

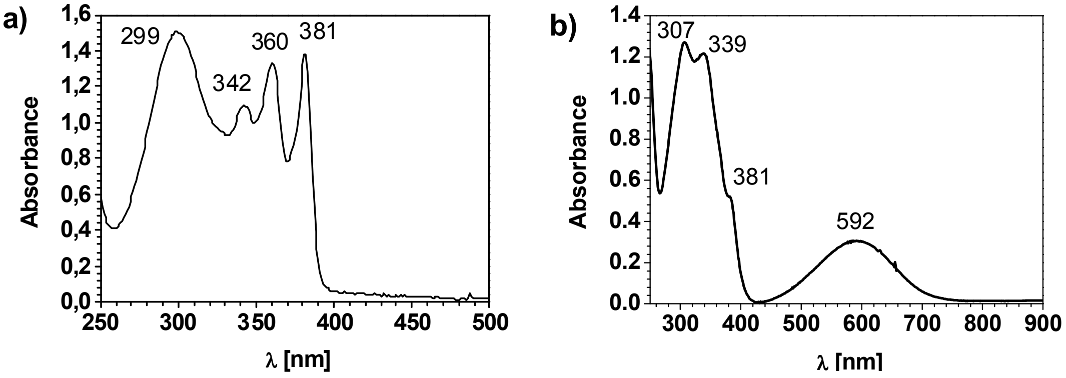

Fig. 2. Solution UV-vis spectra of neutral **B2 (a)** and **B5 (b)** (concentration: 1 × 10^{-4}M in CH_2Cl_2).

Table 3 UV-vis-NIR spectroscopic data obtained for the studied triarylamine-substituted arylene bisimides in their neutral, radical anion, dianion and radical cation states (λ_{max} in nm) in 0.1M Bu_4NPF_6 in CH_2Cl_2 solution

Compound state	**λ_{max} [nm]**
B1 (neutral)	309; 368
B1^{-} (radical anion)	415; 658; 727
B1^{+}(radical cation)	593; 703

B2 (neutral)	299; 342 (*0-2*); 360 (*0-1*); 381 (*0-0*)
B2$^-$ (radical anion)	273; 401; 478; 609; 699; 780
B2^{2-} (dianion)	273; 401; 426; 609
B2$^+$(radical cation)	568; 698
B3 (neutral)	302; 459 (*0-2*); 491 (*0-1*); 527 (*0-0*)
B3$^-$ (radical anion)	682 (*0-3)*; 704 (*0-1*); 714 (*0-0*); 797; 975
B3^{2-} (dianion)	574
B3$^+$(radical cation)	354; 697
B4 (neutral)	300; 342 (*0-2*); 360 (*0-1*); 381 (*0-0*)
B4$^-$ (radical anion)	272; 402; 478; 610; 688; 763
B4^{2-} (dianion)	272; 402; 425; 610
B4$^+$(radical cation)	568; 698
B5 (neutral)	307; 339 (*0-2*); 381 (*0-0*); 592
B5$^-$ (radical anion)	487; 534; 705; 785
B5^{2-} (dianion)	412; 630
B5$^+$(radical cation)	508; 707
B6 (neutral)	307; 339 (*0-2*); 381 (*0-0*); 592
B6$^-$ (radical anion)	487; 534; 705; 785
B6^{2-} (dianion)	412; 630
B6$^+$(radical cation)	502; 535; 684
B7* (neutral)	310; 349; 620
B7$^-$*(radical anion)	303; 485; 530; 703; 785
B7$^+$*(radical cation)	749

**thin solid film spectra*

Spectroelectrochemistry in the reduction mode

In **Fig. 3** UV-vis-NIR spectra of **B2**, registered for decreasing working electrode potentials are collected. The first spectroscopic signs of the electrochemical reduction appear at E=-1.00 V *vs* Fc/Fc$^+$ which almost perfectly coincides with the onset of the first reduction peak in the cyclic voltammogram (-0.97 V *vs* Fc/Fc$^+$, see **Table 1**). Within the potential range of this voltammetric peak (-1.0 V>E>-1.30 V) the following bands attributable to the radical anion form of **B2** appear and grow in intensity: 273 nm; 401 nm, 478 nm, 609 nm, 699 nm reaching the maximum intensity for potentials -1.25 to -1.30 V. They can be unequivocally attributed to the radical anion form of **B2** in accordance with previous findings for arylene bisimides functionalized with non-chromophoric N-substituents.[9,53] For potentials corresponding to the onset of the second reduction peak (-1.35 V) and a potential close to its maximum (-1.50 V) the above listed bands decrease in intensity and a new peak, attributable to the dianion form appears at 426 nm. Concomitantly, the $\pi-\pi*$ band of vibronic character at 381 nm, which is indicative of the neutral form of the bisimide, decreases in intensity over the whole potential range studied.

The triarylamine band at 299 nm does not change its position with decreasing potential, its intensity however increases which may be caused in part by the changing background of the spectrum. It can therefore be concluded that the reduction of **B2** is strictly limited to the bisimide core consistent with the cyclic voltammetry results and previous DFT calculations.[30,31] All bisimides of this group behave similarly, although the positions of their π–π* band as well as the bands corresponding to the radical anion and dianion forms are dependent on the bisimide core size (see Table 3 and Fig. S4 in *Supporting Information*). Similar behaviour has also been reported for an alternating copolymer of naphthalimide and bis(triarylamine), however in this macromolecular compound the vibronic peaks of the bisimide π–π* transition are significantly broadened. This effect, together with a bathochromic shift of the triarylamine peak causes all these bands to nearly merge.[24]

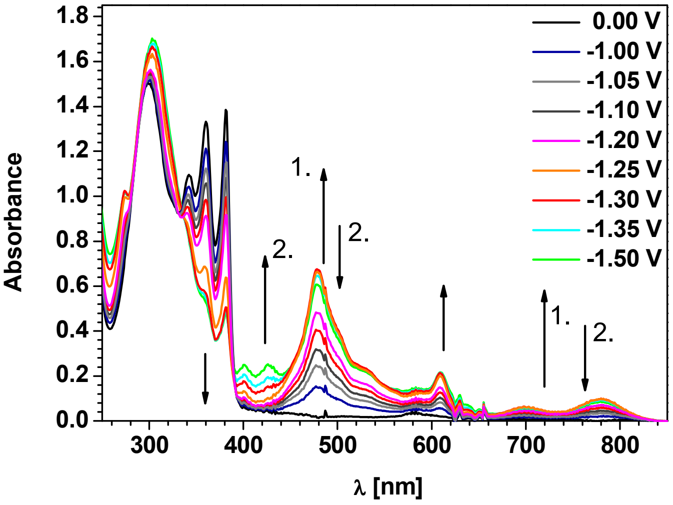

Fig. 3. UV-vis spectra of **B2** registered for decreasing working electrode potential (concentration: 1 × 10^{-4}M**;** electrolyte 0.1M Bu_4NPF_6 in CH_2Cl_2). ↑1. - absorption bands which grow during the first step of reduction; ↑2. - absorption bands which grow during the second step of reduction; ↓2. - absorption bands which decrease during the second step of reduction.

B5 *i.e.* naphthalene bisimide core-substituted with triarylamine is more difficult to reduce than its N-substituted counterpart. Its UV-vis spectrum remains unchanged down to E=-1.10 V *vs* Fc/Fc$^+$. At this potential spectroscopic features characteristic of the radical anion state start to appear (see **Fig. 4**), again in perfect accordance with the onset of the first reduction peak in the cyclic voltammogram of **B5** (compare **Fig. 1b** and **Fig. 4**). In the potentials range covering the first reduction peak in the cyclic voltammogram of **B5** (-1.10 V>E>-1.40 V) the band attributed to the π–π* transition in the bisimide core (at 381 nm (*0-0*) and 339 nm (*0-2*)) decreases in intensity whereas the triarylamine band at 307 nm increases in intensity. Spectral changes above 400 nm are more complicated and their interpretation requires a substantial theoretical support. In particular, it is important to compare theoretically calculated spectra of the neutral and charged forms of **B5.** The calculated spectra (at TDDFT/B3LYP/6-31G(d) level of theory) can be found in **Fig. S8** of *Supporting Information*. The following conclusions can be drawn which are consistent with the experimentally observed spectroelectrochemical behaviour. The CT band at 592 nm in the experimental spectrum undergoes a hypsochromic shift to 484 nm upon the reduction of **B5** to a radical anion. A hypsochromic shift of this band is also found in the calculated spectrum. At lower potentials corresponding to the electrochemical generation of dianions (-1.45 V and -1.50 V) this band diminishes whereas two new bands appear at 412 nm and 630 nm and grow in intensity.

Similar behaviour is found for **B6** (Fig. S5 in *Supporting Information*)**,** however in this case clear spectral changes appear at E = -1.30 V *vs* Fc/Fc$^+$ consistent with the registered cyclic voltammmogram (see **Fig. S1** in *Supporting Information*). Generally in core substituted bisimides both the π–π* band and the CT band are affected, although the position of the reduction induced-bands depends on the size of the bisimide core.[54]

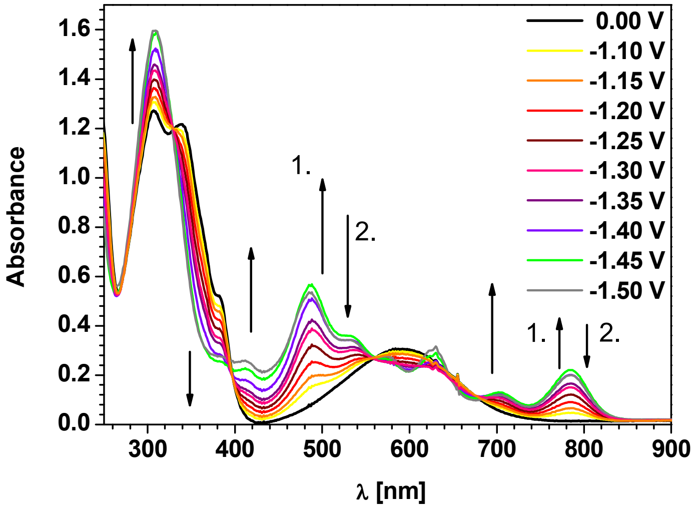

Fig. 4. UV-vis spectra of **B5** registered for decreasing working electrode potential (concentration: 1 × 10^{-4}M**;** electrolyte 0.1M Bu_4NPF_6 in CH_2Cl_2). ↑ 1. - absorption bands which grow during the first step of reduction; ↓ 2. - absorption bands which decrease during the second step of reduction.

Spectroelectrochemical investigations in the solid state were carried out for thin films of the only polymeric bisimide **(B7)**. In **Fig. 5** UV-vis-NIR spectra of this polymer, registered in the potentials range covering the first reduction peak, are collected. In the spectrum of neutral **B7** the π–π* band of the bisimide core is located at 349 nm and shows no vibrational structure. It strongly overlaps with the triarylamine band of λ_{max} at 310 nm. The CT band is bathochromically shifted to 620 nm as compared to the corresponding band in the spectra of the other two core-functionalized bisimides (**B5** and **B6**). The first reduction-induced spectral changes appear at E= -0.95 V *vs* Fc/Fc$^+$ *i.e.* at a potential *ca.* 100 mV higher than the potential of the onset of the of the first reduction peak in the cyclic voltammogram registered for a solution of **B7** in dichloromethane (see **Table 1**). Within the potentials range of the first reduction peak (from -1.05 to -1.30 V) the bisimide band bleaches. The triarylamine band increases in intensity and hypsochromically shifts by 7 nm. The CT band undergoes a hypsochromic shift to 485 nm as predicted in the calculations carried out for its low molecular weight analogue (**B5**). New bands appear at 703 nm and 784 nm.

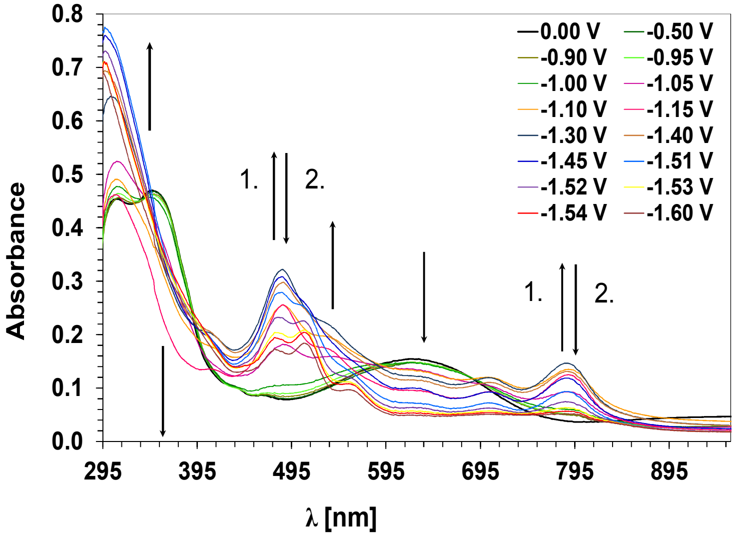

Fig. 5. UV-vis spectra of **B7** registered for decreasing working electrode potential (0.1M Bu_4BF_4/CH_3CN). ↑1. - absorption bands which grow during the first step of reduction; ↑2. - absorption bands which grow during the second step of reduction; ↓2. - absorption bands which decrease during the second step of reduction.

In all studied bisimides stable radical anions can be electrochemically generated by lowering the working electrode potential to the values corresponding to the first reduction peak. In **Fig. 6 a-d** EPR spectra of N-substituted bisimides are compared. Multi-line, well resolved spectra were observed in almost all cases, indicating that no microaggregation of the bisimide occurs during the electrochemical reduction and rapid reorientation of the formed radical anions takes place which results, in turn, in averaging to zero the anisotropic contributions to the *g* factor and to hyperfine interactions.

B1-B4 give multi-line EPR spectra centered at g in the range of 2.0037-2.0047. The observed patterns can be simulated assuming isotropic hyperfine interactions of the unpaired electron with the nuclei of nitrogen atoms and protons of the bisimide core, there is no evidence of the interactions of the unpaired electron with nitrogen atoms or protons of the triarylamine N-substituent**.** The lack of such interactions is additionally corroborated by close similarity of the spectra of **B2** and **B3** to those reported for naphthalene[53] and perylene[17] bisimides N-substituted with alkyl or oligoether groups as well as the similarity of the spectrum of **B4** to that reported for naphthalene bisimide unsymmetrically N-substituted with alkyl and aryl substituents.[55] EPR parameters obtained for the radical anion forms of all bisimides studied are presented in **Table 4** and in greater detail in **Chart S1** of the *Supporting Information*.

Table 4 Fitting parameters for simulation of EPR spectra of radical anions **B1-B6**, together with g-factor estimated from experimental spectra. hfcc – hyperfine coupling constant

Compound	hfcc/G	line width/G	g-factor
B1$^-$	N: 1.18; H: 0.64	0.09	2.0041
B2$^-$	N: 0.93; H: 1.86	0.42	2.0037
B3$^-$	N: 0.57; H: 1.75; 0.61	0.20	2.0039
B4$^-$	N: 0.99; 0.89; H: 1.96; 1.75	0.40	2.0041
B5$^-$	N: 0.88; H: 1.59; 0.23	0.35	2.0047
B6$^-$	N: 1.35, 1.05, 1.12; H: 4.04, 1.01, 0.9, 0.7	0.40	2.0046
B7$^-$	-	-	2.0039

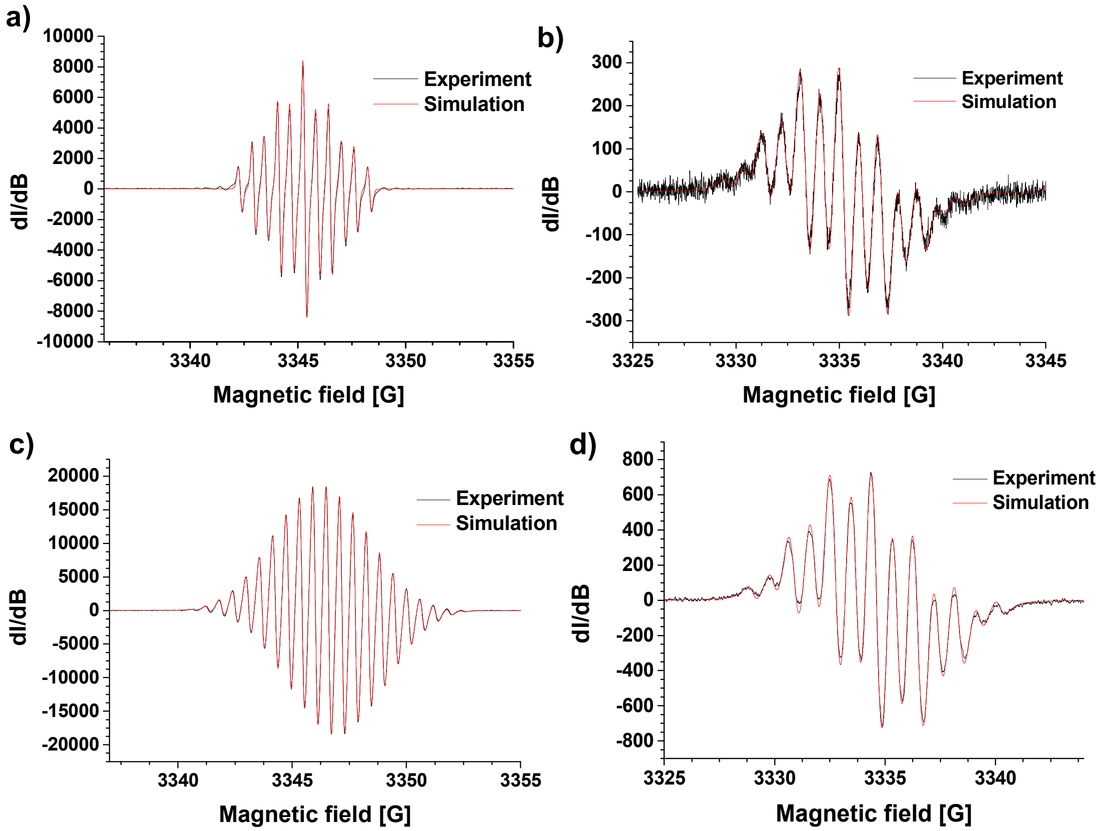

Fig. 6. Experimental and simulated EPR spectra of electrochemically generated radical anions of arylene bisimides N-substituted with triarylamine (1 × 10^{-3}M**;** electrolyte 0.1M Bu_4NPF_6 in CH_2Cl_2): a) **B1** (E = -1.2 V); b) **B2** (E = -1.0 V); c) **B3** (E = -1.0 V); d) **B4** (E = -1.0 V). Modulation width in range of 0.01-0.05G; microwave power 1mW. Fitting parameters can be found in *Supporting Information* (Chart S1).

As judged from the coupling constants, in the symmetrically N-substituted bisimides (**B1,B2** and **B3**) the maximum spin density of the unpaired electron is located in the center of the arylene core; in the asymmetric derivative **(B4)** it is slightly displaced towards this half of the core which is connected to the triarylamine moiety.

EPR spectra of core-functionalized bisimides are shown in **Fig. 7** whereas the corresponding spectral parameters are listed in **Table 4** and in **Chart S1** of the *Supporting Information.*

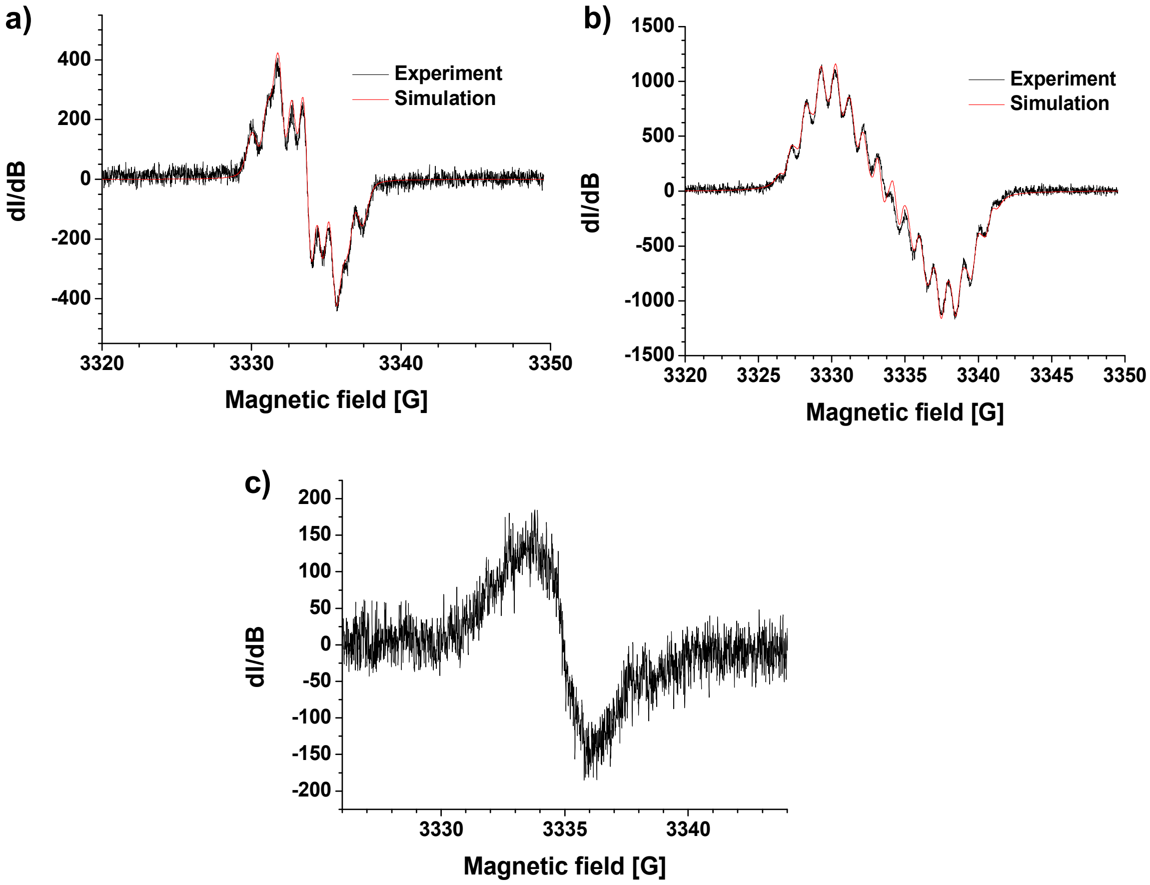

Fig. 7. Experimental and simulated EPR spectra of electrochemically generated radical anions of arylene bisimides core-substituted with triarylamine (1×10^{-3}M**;** electrolyte 0.1M Bu_4NPF_6 in CH_2Cl_2: a) **B5** (E = -1.1 V); b) **B6** (E = -1.3 V); c) **B7** (E = -1.1 V). Modulation width in range of 0.01-0.05G; microwave power 1mW. Fitting parameters can be found in *Supporting Information* (Chart S1).

From the set of the coupling constants obtained for **B5** *i.e.* symmetrically core-disubstituted naphthalene bisimide, it can be concluded that similarly as in **B2** – its N-substituted counterpart – the maximum spin density of the unpaired electron is located in the center of the aromatic core. **B6** is an interesting case since it contains two non-equivalent substituents, one of them being attached to the core *via* amine-type nitrogen. The electron donating effect of this substituent has a profound effect on the distribution of the unpaired electron spin density whose maximum is displaced to this part of the aromatic core which is the most distant from the amine substituent (note the significantly enhanced coupling constant for H1, chart **S1** in *Supporting Information*). A similar phenomenon was previously reported for perylene bisimides core-functionalized with secondary amines.[54] Different behaviour was observed for **B7**. As a macromolecular equivalent of **B5,** it should exhibit similar EPR spectral parameters. However, only a single broad signal with no hyperfine splitting was recorded. This probably results from the higher molecular weight of this compound, which could lead to aggregation of charged polymer chains. No model was proposed here since many different combinations can be fitted into this spectrum.

To summarize this part of the work, arylene bisimides N- and core-substituted with triarylamine show very interesting electrochemistry in the reduction mode. They undergo *quasi*-reversible reduction at relatively high potentials yielding radical anions which show excellent stability at room temperature. Moreover, the presence of an additional chromophore (triarylamine), makes the spectroelectrochemical behaviour of these compounds distinctly different from that reported for arylene bisimides which do not contain chromophoric substituents.

Spectroelectrochemistry in the oxidation mode

Low and high molecular weight triaryl- or bis(triarylamine)-functionalized bisimides show an interesting spectroelectrochemical behaviour not only in the reduction but also in the oxidation mode, associated with their *quasi*-reversible oxidation of their triarylamine parts to radical cations. Polymeric electrochromic devices showing high optical contrast based on this family of compounds have been proposed.[24,27,28] In **Fig. 8** UV-vis spectra of **B2**, registered for increasing working electrode potentials are shown as a representative example of the spectroelectrochemical behaviour of N-functionalized bisimides studied in this research. The remaining–bisimides of this group **(B1, B3, B4)** behave in a similar manner, their spectra registered at different potentials can be found in **Fig. S6** of *Supporting Information.* Position of the peaks characteristic of the radical cations formed are listed in **Table 3.**

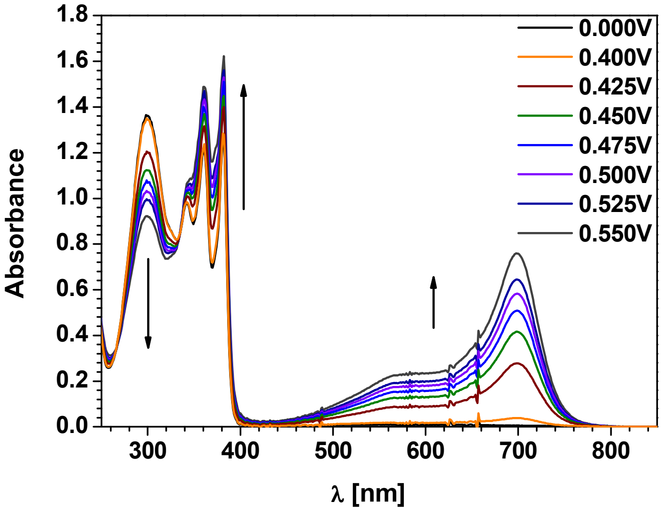

Fig. 8. UV-vis spectra of **B2** registered for increasing working electrode potential (concentration: 1 × 10^{-4}M**;** electrolyte 0.1M Bu_4NPF_6 in CH_2Cl_2).

Electrochemical oxidation of N-substituted bisimides gives rise to a profound decrease of the band at *ca.* 300 nm, characteristic of the neutral triarylamine moiety with simultaneous increase of two radical cation-originating bands at 568 nm and 698 nm. The bisimide band of vibronic character does not undergo significant changes, apart from slight broadening and slight increase of intensity. This means that the lowering of the electron density caused by the oxidation is limited to the triarylamine moiety, consistent with the previous DFT calculations.[30,31] The observed spectral changes induced by increasing polarization of the working electrode are similar to previous results reporting spectroelectrochemical investigations of the oxidation of triarylamines linked together by a conjugated bridge[56–62] Bisimides core-substituted with triarylamine are more difficult to oxidize than the N-substituted ones (see **Table 2**). Consistent with the cyclic voltammetry studies, the first signs of their oxidation appear at potentials higher by *ca.* 50 to 90 mV as compared to the case of N-substituted bisimides. **Fig. 9** shows the spectra of **B5** registered at the increasing working electrode potentials. The corresponding spectra of **B6** can be found in the *Supporting Information.*

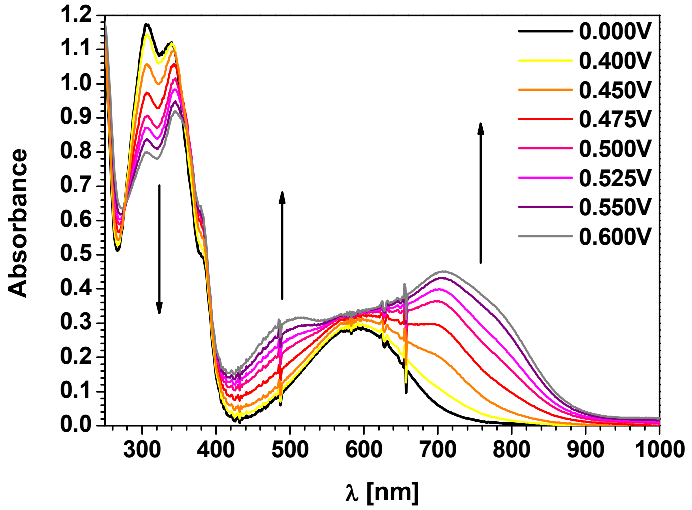

Fig. 9. UV-vis spectra of **B5** registered for increasing working electrode potential (concentration: 1 × 10^{-4}M**;** electrolyte 0.1M Bu_4NPF_6 in CH_2Cl_2).

Upon oxidation of **B5** the band at 307 nm, characteristic of neutral triarylamine moiety quickly decreases with increasing electrode potential. The bisimide band at 339 nm is essentially unaffected by the oxidation, apart from an apparent decrease of its intensity caused by its partial superposition on the disappearing triarylamine band. Other changes in the UV-vis spectra are also present. The CT band at 592 nm in the experimental spectrum undergoes a hypsochromic shift to 512 nm. In addition new bands ascribed to various transitions in the radical cation form appear at a less energetic part of the spectrum. Consistent with the experimental spectrum, an oxidation induced hypsochromic shift of the CT band is also clearly seen in the calculated spectrum (see Fig. S8 in *Supporting Information*). The spectroelectrochemical behaviour of **B6** is similar (see Fig. S7 in *Supporting Information*).

Spectroelectrochemical investigations in the solid state were carried out for thin films of **B7**. The resulting spectra are shown in **Fig. 10**. The observed behaviour is similar as that observed for **B5** – disappearance of the triarylamine band at 313 nm and growth of a new band at 749 nm ascribed to the radical cation form of triarylamine which is superimposed on the CT band undergoing hypsochromic shift upon increasing electrode potential. The bands are however significantly broader, as frequently observed for the solid state spectra.

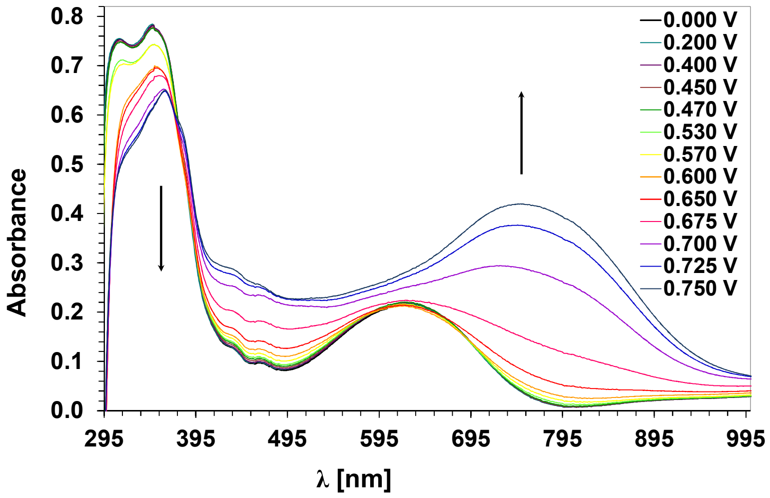

Fig. 10. UV-vis spectra of a thin film of **B7** registered for increasing working electrode potential (electrolyte 0.1M Bu_4BF_4/CH_3CN).

In all studied bisimides functionalized with triarylamine stable radical cations can be electrochemically generated. EPR spectra of the radical cation forms of **B1-B4** are presented in **Fig.12 a-d**.

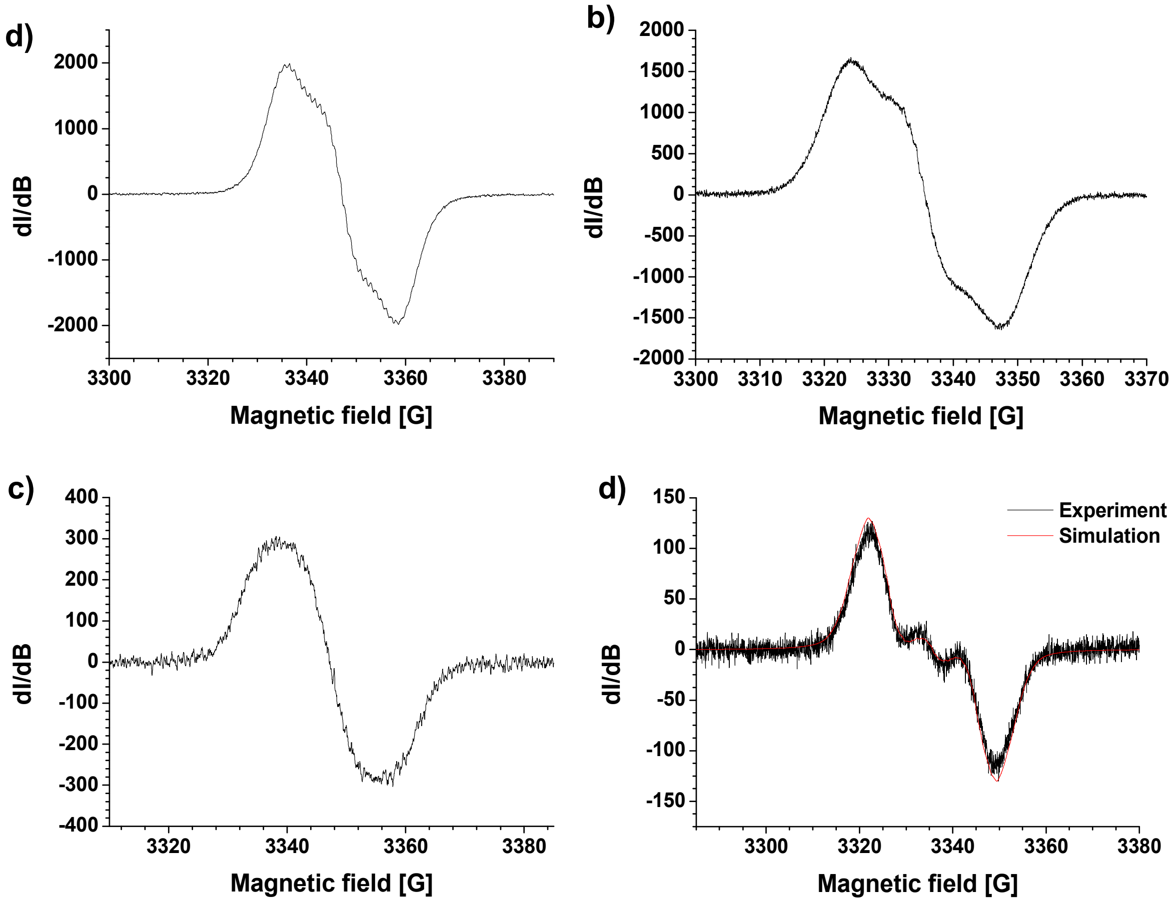

Fig. 12. Experimental and simulated (in the case of **B4**) EPR spectra of electrochemically generated radical cations of arylene bisimides N-substituted with triarylamine **(**1 × 10^{-3}M**;** electrolyte 0.1M Bu_4NPF_6 in CH_2Cl_2)**:** a) **B1** (E = 0.5 V); b) **B2** (E = 0.5 V); c) **B3** (E = 0.5 V); d) **B4** (E = 0.5 V). Modulation width in range of 0.1 - 0.6 G; microwave power 1mW. Fitting parameters for **B4** can be found in *Supporting Information* (**Chart S2**).

As judged from the corresponding cyclic voltammograms in **B1**, **B2** and **B3** radical cations are formed on each triarylamine substituent at the same potential since the area under the peaks of the redox couple corresponding to the oxidation of these bisimides to the radical cation form is twice as high than the area under the peaks ascribed to the redox couple originating from the monoelectronic reduction of these bisimides to radical anions (see **Fig. 1a** and **Fig. S1** in the *Supporting Information*). All three compounds can be considered as two triarylamine moieties connected by a non-conjugated bridge. The formation of stable dications of diradical character in this type of compounds is known,[49,63–65] however the formation of such paramagnetic moieties in triarylamines connected by a conjugated linker has also been recently reported.[66]

Table 5 g-factors of radical cations of core-substituted bisimides

Compound	g-factor
B1$^+$	2.0037
B2$^+$	2.0037
B3$^+$	2.0037
B4$^+$	2.0038
B5$^+$	2.0036
B6$^+$	2.0038
B7$^+$	2.0036

Core-functionalized bisimides (**B5**, **B6** and **B7**) also form stable radical cations which can be electrochemically generated and detected in an EPR spectroelectrochemical experiment. Their EPR spectra are shown in **Fig. 12 a-c.** The spectra of radical cations of triarylamine fuctionalized arylene bisimides are less resolved as compared to the spectra of the corresponding radical anions. This is caused by the fact that in the trirylamine substituent a larger number of protons contribute to the hyperfine interaction which results in a strong overlap of individual lines and the overall line broadening**.** The shape of the EPR spectra is further disturbed by a somehow diradical character of the oxidized forms of **B1**, **B2** and **B3.** This is clearly seen when one compares the spectra of **B2** and **B4** radical cations**.** In the case of **B4** a partially resolved three-line spectrum is observed, while in **B2** with two triphenylamine substituents a single broad line is seen as an effect of interactions between two unpaired spins. The obtained coupling constants for **B4** seem to indicate that the maximum spin density of the unpaired electron is predominantly located on the amine nitrogen and to a lesser extent on the two alkyl-substituted rings. Smaller spin density of the unpaired electron is found on the disubstituted (phenylene) ring (*Supporting Information* **chart S2**). Thus, the unpaired electron spin density is displaced in such a manner as to be distant from the bisimide core. Poorly resolved spectra of core substituted bisimides are difficult to interpret. However, based on the value of their g-factor (see **table 5**), which is similar to that found for the N-substituted bisimides, **B1-B4,** and to the earlier reported g-factor of the triphenylamine radical cation,[67] it can be postulated that in the case of core substituted bisimides, **B5-B7**, the majority of the spin density is localized on the triphenylamine moiety.

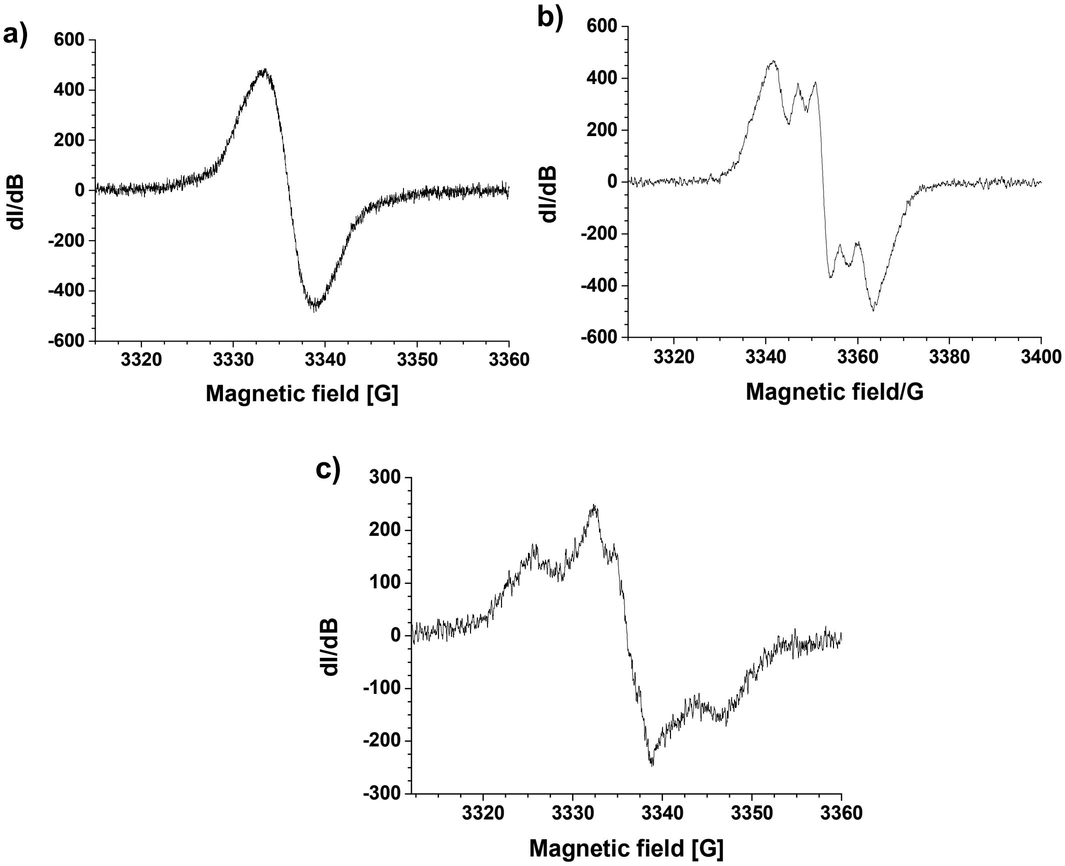

Fig. 13. Experimental EPR spectra of electrochemically generated radical cations of arylene bisimides N-substituted with triarylamine (1 × 10^{-3} M**;** electrolyte 0.1M Bu_4NPF_6 in CH_2Cl_2): a) **B5** (E = 0.55 V); b) **B6** (E = 0.5 V); c) **B7** (E = 0.5 V). Modulation width in range of 0.1 - 0.6G; microwave power 1 mW.

To summarize the second part of the work, both N- and core-substituted bisimides of low molecular weight undergo *quasi*-reversible oxidation ascribed to the formation of stable radical cations, detectable by EPR at the triarylamine substituents. The presence of these radicals give rise to profound spectroscopic changes in the UV-vis-NIR region, distinctly different from the changes induced by electrochemical reduction of these compounds. Electrochemical oxidation of the polymeric core-functionalized bisimide is less reversible.

Conclusions

To conclude, we have studied the spectroelectrochemical behaviour of a series of arylene bisimides N- and core-substituted with triarylamine. Some of these compounds were previously investigated as components of ambipolar[17,31] and p-channel[30] field effect transistors. EPR spectroelectrochemical investigations confirmed ambipolarity of these compounds demonstrating the formation of stable radical anions upon *quasi*-reversible one-electron reduction and stable radical cations upon quasi-reversible oxidation. Both redox processes involve profound and distinctly different spectral changes in the visible range of the spectrum demonstrating their promising multicolor electrochromism.

Acknowledgements

This research was supported in part by PL-Grid Infrastructure. S. Pluczyk and P. Zassowski are scholars supported by the "Doktoris–scholarship program for an innovative Silesia", co-financed by European Union within European Social Fund. The presented research was also financed by the project entitled "New solution processable organic and hybrid (organic/inorganic) functional materials for electronics, optoelectronics and spintronics" (Contract no. TEAM/2011–8/6), which is operated within the Foundation for the Polish Science Team Programme, cofinanced by the EU European Regional Development Fund (M.Z. and A.P.) and by Polish-Norwegian Research Programme operated by the National Centre for Research and Development under the Norwegian Financial Mechanism 2009-2014 in the frame of Project Contract No Pol-Nor/210704/43/2013 R.R). R.R. additionally acknowledges the support of the Foundation for Polish Science within the framework of START 2014 Programme.

Notes and references

1. Z. Chen, A. Lohr, C. R. Saha-Möller, and F. Würthner, *Chem. Soc. Rev.*, 2009, **38**, 564–84.
2. C. Huang, S. Barlow, and S. R. Marder, *J. Org. Chem.*, 2011, **76**, 2386–407.
3. A. N. Sokolov, M. E. Roberts, O. B. Johnson, Y. Cao, and Z. Bao, *Adv. Mater.*, 2010, **22**, 2349–53.
4. J. E. Anthony, A. Facchetti, M. Heeney, S. R. Marder, and X. Zhan, *Adv. Mater.*, 2010, **22**, 3876–92.
5. X. Zhan, A. Facchetti, S. Barlow, T. J. Marks, M. A. Ratner, M. R. Wasielewski, and S. R. Marder, *Adv. Mater.*, 2011, **23**, 268–84.
6. F. Würthner and M. Stolte, *Chem. Commun. (Camb).*, 2011, **47**, 5109–15.
7. R. Rybakiewicz, I. Tszydel, J. Zapala, L. Skorka, D. Wamil, D. Djurado, J. Pécaut, J. Ulanski, M. Zagorska, and A. Pron, *RSC Adv.*, 2014, **4**, 14089.
8. Q. Meng and W. Hu, *Phys. Chem. Chem. Phys.*, 2012, **14**, 14152–64.
9. C. R. Wade, M. Li, and M. Dincă, *Angew. Chem. Int. Ed. Engl.*, 2013, **52**, 13377–81.
10. G.-B. Li, L. Li, J.-M. Liu, T. Yang, and C.-Y. Su, *Cryst. Growth Des.*, 2013, **13**, 1518–1525.

11. C. F. Leong, T. B. Faust, P. Turner, P. M. Usov, C. J. Kepert, R. Babarao, A. W. Thornton, and D. M. D'Alessandro, *Dalton Trans.*, 2013, **42**, 9831–9.

12. L. Han, L. Qin, L. Xu, Y. Zhou, J. Sun, and X. Zou, *Chem. Commun. (Camb).*, 2013, **49**, 406–8.

13. P. M. Usov, C. Fabian, and D. M. D'Alessandro, *Chem. Commun. (Camb).*, 2012, **48**, 3945–7.

14. R. Schmidt, J. H. Oh, Y.-S. Sun, M. Deppisch, A.-M. Krause, K. Radacki, H. Braunschweig, M. Könemann, P. Erk, Z. Bao, and F. Würthner, *J. Am. Chem. Soc.*, 2009, **131**, 6215–28.

15. H. Katz, A. Lovinger, J. Johnson, C. Kloc, T. Siegrist, W. Li, Y. Lin, and A. Dodabalapur, *Nature*, 2000, **404**, 478–81.

16. H. E. Katz, J. Johnson, A. J. Lovinger, and W. Li, *J. Am. Chem. Soc.*, 2000, **122**, 7787–7792.

17. A. Pron, R. R. Reghu, R. Rybakiewicz, H. Cybulski, D. Djurado, J. V. Grazulevicius, M. Zagorska, I. Kulszewicz-Bajer, and J.-M. Verilhac, *J. Phys. Chem. C*, 2011, **115**, 15008–15017.

18. Y. Ma, Y. Wu, Y. Zhao, H. Fu, and J. Yao, *Phys. Chem. Chem. Phys.*, 2011, **13**, 2036–43.

19. A. Pron, P. Gawrys, M. Zagorska, D. Djurado, and R. Demadrille, *Chem. Soc. Rev.*, 2010, **39**, 2577–2632.

20. T. Lana-Villarreal, J. M. Campiña, N. Guijarro, and R. Gómez, *Phys. Chem. Chem. Phys.*, 2011, **13**, 4013–21.

21. C. Quinton, V. Alain-Rizzo, C. Dumas-Verdes, F. Miomandre, G. Clavier, and P. Audebert, *RSC Adv.*, 2014, **4**, 34332.

22. P. Bujak, I. Kulszewicz-Bajer, M. Zagorska, V. Maurel, I. Wielgus, and A. Pron, *Chem. Soc. Rev.*, 2013, **42**, 8895–999.

23. H.-J. Yen, C.-J. Chen, and G.-S. Liou, *Adv. Funct. Mater.*, 2013, **23**, 5307–5316.

24. H.-M. Wang and S.-H. Hsiao, *J. Mater. Chem. C*, 2014, **2**, 1553.

25. H.-M. Wang and S.-H. Hsiao, *J. Polym. Sci. Part A Polym. Chem.*, 2014, **52**, 1172–1184.

26. T. Kurosawa, Y.-C. Lai, T. Higashihara, M. Ueda, C.-L. Liu, and W.-C. Chen, *Macromolecules*, 2012, **45**, 4556–4563.

27. H.-M. Wang and S.-H. Hsiao, *Polymer (Guildf).*, 2009, **50**, 1692–1699.

28. H.-J. Yen and G.-S. Liou, *Polym. Chem.*, 2012, **3**, 255.

29. A. Iwan and D. Sek, *Prog. Polym. Sci.*, 2011, **36**, 1277–1325.

30. R. Rybakiewicz, D. Djurado, H. Cybulski, E. Dobrzynska, I. Kulszewicz-Bajer, D. Boudinet, J.-M. Verilhac, M. Zagorska, and A. Pron, *Synth. Met.*, 2011, **161**, 1600–1610.

31. R. Rybakiewicz, J. Zapala, D. Djurado, R. Nowakowski, P. Toman, J. Pfleger, J.-M. Verilhac, M. Zagorska, and A. Pron, *Phys. Chem. Chem. Phys.*, 2013, **15**, 1578–87.

32. R. Rybakiewicz, P. Gawrys, D. Tsikritzis, K. Emmanouil, S. Kennou, M. Zagorska, and A. Pron, *Electrochim. Acta*, 2013, **96**, 13–17.

33. C. M. Dufft and G. A. Heath, *Inorg. Chem.*, 1991, **30**, 2528–2535.

34. W . Kaim and A. Klein (Eds.) *Spectroelectrochemistry*, Royal Society of Chemistry, 2008.

35. S. A. Macgregor, E. M. R. J. Sorbie, and L. J. Yellowlees in A. J. L. Pomberio and J. A. McCleverty (Eds.), *Molecular Electrochemistry of Inorganic, Bioinorganic and Organometallic Comounds* 1993, 503–517.

36. L. P. Moorcraft, A. Morandeira, J. R. Durrant, J. R. Jennings, L. M. Peter, S. Parsons, A. Turner, J. Yellowlees, and N. Robertson, *Dalt. Trans.*, 2008, **2**, 6940–6947.

37. D. N. Mason, G. B. Deacon, J. Yellowlees, and A. M. Bond, *Dalt. Trans.*, 2003, 890–900.

38. P. R. Murray, D. Collison, S. Daff, N. Austin, R. Edge, B. W. Flynn, L. Jack, F. Leroux, E. J. L. Mcinnes, A. F. Murray, D. Sells, T. Stevenson, J. Wolowska, and L. J. Yellowlees, *J. Magn. Reson.*, 2011, **213**, 206–209.

39. A. Zykwinska, W. Domagala, A. Czardybon, B. Pilawa, and M. Lapkowski, *Electrochim. Acta*, 2006, **51**, 2135–2144.

40. D. R. Duling, *J. Magn. Reson. Ser. B*, 1994, **104**, 105–110.

41. A. D. Becke, *J. Chem. Phys.*, 1993, **98**, 1372.

42. C. Lee, W. Yang, and R. G. Parr, *Phys. Rev. B*, 1988, **37**, 785–789.

43. A. D. Becke, *J. Chem. Phys.*, 1993, **98**, 5648–5652.

44. J. Tomasi, B. Mennucci, and R. Cammi, *Chem. Rev.*, 2005, **105**, 2999–3093.

45. Gaussian 09, Revision D.01, M. J. Frisch, G. W. Trucks, H. B. Schlegel, G. E. Scuseria, M. A. Robb, J. R. Cheeseman, G. Scalmani, V. Barone, B. Mennucci, G. A. Petersson, H. Nakatsuji, M. Caricato, X. Li, H. P. Hratchian, A. F. Izmaylov, J. Bloino, G. Zheng, J. L. Sonnenberg, M. Hada, M. Ehara, K. Toyota, R. Fukuda, J. Hasegawa,

M. Ishida, T. Nakajima, Y. Honda, O. Kitao, H. Nakai, T. Vreven, J. A. Montgomery, Jr., J. E. Peralta, F. Ogliaro, M. Bearpark, J. J. Heyd, E. Brothers, K. N. Kudin, V. N. Staroverov, R. Kobayashi, J. Normand, K. Raghavachari, A. Rendell, J. C. Burant, S. S. Iyengar, J. Tomasi, M. Cossi, N. Rega, J. M. Millam, M. Klene, J. E. Knox, J. B. Cross, V. Bakken, C. Adamo, J. Jaramillo, R. Gomperts, R. E. Stratmann, O. Yazyev, A. J. Austin, R. Cammi, C. Pomelli, J. W. Ochterski, R. L. Martin, K. Morokuma, V. G. Zakrzewski, G. A. Voth, P. Salvador, J. J. Dannenberg, S. Dapprich, A. D. Daniels, Ö. Farkas, J. B. Foresman, J. V. Ortiz, J. Cioslowski, and D. J. Fox, Gaussian, Inc., Wallingford CT, 2009.

46. A.-R. Allouche, *J. Comput. Chem.*, 2011, **32**, 174–82.

47. S. K. Lee, Y. Zu, A. Herrmann, Y. Geerts, K. Müllen, and A. J. Bard, *J. Am. Chem. Soc.*, 1999, **121**, 3513–3520.

48. H. Wu, H. Wang, L. Xue, Y. Shi, and X. Li, *J. Phys. Chem. B*, 2010, **114**, 14420–5.

49. Z. An, S. A. Odom, R. F. Kelley, C. Huang, X. Zhang, S. Barlow, L. A. Padilha, J. Fu, S. Webster, D. J. Hagan, E. W. Van Stryland, M. R. Wasielewski, and S. R. Marder, *J. Phys. Chem. A*, 2009, **113**, 5585–93.

50. M. Velusamy, J.-Y. Shen, J. T. Lin, Y.-C. Lin, C.-C. Hsieh, C.-H. Lai, C.-W. Lai, M.-L. Ho, Y.-C. Chen, P.-T. Chou, and J.-K. Hsiao, *Adv. Funct. Mater.*, 2009, **19**, 2388–2397.

51. C.-C. Lin, M. Velusamy, H.-H. Chou, J. T. Lin, and P.-T. Chou, *Tetrahedron*, 2010, **66**, 8629–8634.

52. C.-C. Chao, M. Leung, Y. O. Su, K.-Y. Chiu, T.-H. Lin, S.-J. Shieh, and S.-C. Lin, *J. Org. Chem.*, 2005, **70**, 4323–31.

53. G. Andric, J. F. Boas, A. M. Bond, G. D. Fallon, K. P. Ghiggino, C. F. Hogan, J. A. Hutchison, M. A.-P. Lee, S. J. Langford, J. R. Pilbrow, G. J. Troup, and C. P. Woodward, *Aust. J. Chem.*, 2004, **57**, 1011.

54. M. J. Ahrens, M. J. Tauber, and M. R. Wasielewski, *J. Org. Chem.*, 2006, **71**, 2107–14.

55. A.-J. Avestro, D. M. Gardner, N. A. Vermeulen, E. A. Wilson, S. T. Schneebeli, A. C. Whalley, M. E. Belowich, R. Carmieli, M. R. Wasielewski, and J. F. Stoddart, *Angew. Chem. Int. Ed. Engl.*, 2014, **53**, 4442–9.

56. S. Barlow, C. Risko, S. Chung, N. M. Tucker, V. Coropceanu, S. C. Jones, Z. Levi, J. Bre, and S. R. Marder, *J. Am. Chem. Soc.*, 2005, **127**, 16900–16911.

57. P. J. Low, M. A. J. Paterson, H. Puschmann, A. E. Goeta, A. K. Howard, C. Lambert, J. C. Cherryman, D. R. Tackley, S. Leeming, and B. Brown, *Chem. Eur. J.*, 2004, **10**, 83–91.

58. C. Lambert and S. Amthor, *J. Phys. Chem. A*, 2004, **108**, 6474–6486.

59. C. Lambert and G. Nöll, *J. Am. Chem. Soc.*, 1999, **121**, 8434–8442.

60. J. M. Chem, C. Huang, M. M. Sartin, N. Siegel, M. Cozzuol, Y. Zhang, J. M. Hales, S. Barlow, J. W. Perry, and S. R. Marder, *J.ournal Mater. Chem.*, 2011, **21**, 16119–16128.

61. M. Oyama, K. Nozaki, and S. Okazaki, *Anal. Chem.*, 1991, **63**, 1387–1392.

62. Lambert, Christoph, G. Nöll, and J. Schelter, *Nat. Mater.*, 2002, **1**, 69.

63. A. Ito, M. Urabe, and K. Tanaka, *Angew. Chemie Int. Ed.*, 2009, **48**, 5785–5785.

64. Y. Yokoyama, D. Sakamaki, A. Ito, K. Tanaka, and M. Shiro, *Angew. Chem. Int. Ed. Engl.*, 2012, **51**, 9403–6.

65. C. L. Ramírez, C. Pegoraro, L. Trupp, A. Bruttomesso, V. Amorebieta, D. M. A. Vera, and A. R. Parise, *Phys. Chem. Chem. Phys.*, 2011, **13**, 20076–80.

66. Y. Su, X. Wang, X. Zheng, Z. Zhang, Y. Song, Y. Sui, Y. Li, and X. Wang, *Angew. Chemie*, 2014, **126**, 2901–2905.

67. T. Nagai, K. Katayama, and N. Tokura, *Chem. Lett.*, 1973, 919–922.